Impact of the elemental composition of exported organic matter on the observed dissolved nutrient and trace element distributions in the upper layer of the ocean

Author

Paul Quay

School of Oceanography

MS 355351

University of Washington

Seattle, WA 98195

206-685-8061

pdquay@uw.edu

ORCID: https://orcid.org/0000-0001-5147-0289

Key Points

- Variations in nutrient distributions in upper ocean result from C/N/P of exported organic matter, nitrogen fixation and air-sea CO_2 flux.
- Nutrient and trace element (TE) budgets yield estimates of the C/N/P/TE composition of exported organic matter (OM) from surface ocean.
- Estimated C/N/P of exported OM has maxima in the subtropics well above Redfield which agree with observations and modeling results.

Abstract

Systematic regional variations in the ratio of nutrient depth gradients of dissolved inorganic carbon (ΔDIC): nitrate (ΔNO_3): phosphate (ΔPO_4) in the upper layer (300m) of the Pacific Ocean are observed. Regional variations in the $\Delta DIC/\Delta NO_3/\Delta PO_4$ are primarily the result of three processes, that is, the C/N/P of organic matter (OM) being exported and subsequently degraded, nitrogen fixation and air-sea CO_2 gas exchange. The link between the observed dissolved $\Delta DIC/\Delta NO_3/\Delta PO_4$ and the C/N/P of exported OM is established using surface layer dissolved DIC, NO_3 and PO_4 budgets. These budgets, in turn, provide a means to indirectly estimate the C/N/P of OM being exported from the surface layer of the ocean. The indirectly estimated C/N/P of exported OM reach maxima in the subtropical gyres at 177/22/1 that is significantly greater than the Redfield ratio and a minimum in the equatorial ocean at 109/16/1 with both results agreeing with available observed particle C/N/P and ocean biogeochemical models. The budget approach was applied to a bioactive trace element (TE) using the measured dissolved Cadmium (Cd) to PO_4 gradients to estimate the Cd/P of exported OM in the Pacific Ocean. Combining the budget method with the availability of high-quality dissolved nutrient and trace element data collected during the GOSHIP and GEOTRACES programs could potentially provide estimates of the C/N/P/TE of exported OM on global ocean scales which would significantly improve our understanding of the link between the ocean's biological pump and dissolved nutrient distributions in the upper ocean.

Plain Language Summary

Microscopic plants in the surface ocean called phytoplankton use photosynthesis to convert carbon dioxide (CO_2) into organic compounds like carbohydrates, fats and proteins. When phytoplankton die or are eaten by small animals (zooplankton) most of these compounds are consumed for energy. A small fraction of the organic compounds in phytoplankton escape consumption and sink into deeper portions of the ocean. This sinking organic matter is consumed as food by bacteria and ultimately released as inorganic compounds like CO_2, nitrate (NO_3) and phosphate (PO_4). The ratio at which CO_2, NO_3 and PO_4 is released depends on the

ratio of carbon (C):nitrogen (N):phosphorous (P) of the sinking organic matter and is a critical factor in determining the distribution of nutrients (CO_2, NO_3, PO_4) in the upper ocean. However, there are very few direct measurements of the C:N:P of sinking organic matter. In this study, a new method is presented to estimate the C:N:P of sinking organic matter based on the observed distributions of CO_2, NO_3 and PO_4 in the upper ocean. This method can potentially estimate the C:N:P of sinking organic matter on a global scale and improve our understanding of the processes that control the distribution of nutrients in the ocean.

Keywords: nutrient cycling, carbon cycling, phytoplankton, trace elements.

1. Introduction

The ocean's biological pump describes the transfer or export of organic matter (OM) out of the surface photic layer of the ocean into the deeper layers of the aphotic ocean. OM export and its subsequent degradation in the aphotic ocean has a major impact on the depth distributions of dissolved nutrients, oxygen, CO_2 and bioactive trace elements in the ocean. Furthermore, the ocean's biological pump is a means to sequester CO_2 in the deep ocean and thus is a key component of the earth's CO_2 cycle. Despite the importance of the ocean's biological pump surprisingly little is known about variations in the elemental composition of the OM being exported which has often resulted in an assumption that the elemental ratio of exported OM has a constant carbon (C): nitrogen (N): phosphorous (P) ratio following the classic Redfield C/N/P ratio of 106:16:1 (Redfield, 1958). However, there have been an increasing number of ocean biogeochemical modeling studies that indicate that the element composition of particles in the surface ocean deviate significant from Redfield (e.g., Weber and Deutsch, 2010; Deutsch and Weber, 2012; Teng et al., 2014, Wang et al., 2019). Yet, it has been difficult to validate these model results for several reasons. First, regional coverage by existing data is poor with most of the ocean being unsampled (e.g., Martiny et al., 2013). Second, a two-fold short term variability of the measured C/N/P of suspended particles at sites is typical (e.g., Karl et al., 2001; Bishop and Wood, 2008). Third, the C/N/P of suspended particles does not necessarily represent the C/N/P exported OM because of differential sinking rates of particles and a significant fraction (~20%) of the exported OM being in the dissolved phase (Hansell et al., 2007). Our current lack of knowledge about the elemental composition of exported OM leaves a substantial gap in our understanding of the ocean's biological pump and its role in controlling dissolved nutrient distributions in the mesopelagic zone (200-1000m) of the ocean.

Even with the limited data on the C/N/P of suspended particles in the surface ocean there are some significant regional trends. Martiny et al. (2013) compiled ~5000 particle C/N/P measurements and found the highest C/P of 170-230 and N/P of 25-37 occurred in the nutrient depleted subtropical gyres and significantly lower C/P of 119-137 and N/P of 14-18 occurred in the nutrient replete subpolar and equatorial regions. Martiny et al. (2013) concluded that this spatial pattern is driven in large part by shifts in plankton assemblages with the cyanobacteria that dominate the oligotrophic gyres having a substantially higher C/P (161-235) and N/P (25-

35) than eukaryotes with C/N/P of 107/16/1 that are more dominant in nutrient replete regions. Martiny et al. found an overall mean C/N/P for particles of 146:20:1which is significantly higher than Redfield. As pointed out previously, the higher the C/N/P of exported OM the greater the potential of the biological pump to sequester CO_2 from the atmosphere (e.g., Martiny et al., 2013, Teng et al., 2014).

The greatest impact of OM degradation occurs in the shallowest layers of the thermocline just below the photic layer where the OM flux is greatest and degradation rates are highest. Vertical flux of sinking particles measured in the subtropical and subpolar N. Pacific Ocean showed that 50-75% of particles were degraded within the upper 300m (Martin, 1987). Quay and Wu (2015) showed that within the upper layers (<300m) of the N. Atlantic Ocean the slope of nitrate versus phosphate concentrations ($\Delta NO_3/\Delta PO_4$) was 16±0.2. However, deeper in the thermocline (500-1500m) the $\Delta NO_3/\Delta PO_4$ decreased to 14.6±0.2 and was close to the $\Delta NO_3/\Delta PO_4$ expected by conservative water mass mixing between Mediterranean Water and Antarctic Intermediate Water and at depths >2000m the observed $\Delta NO_3/\Delta PO_4$ was 13±0.4 and equaled the $\Delta NO_3/\Delta PO_4$ expected by conservative water mass mixing between North Atlantic Deep Water and Antarctic Bottom Water with little apparent impact by in situ OM degradation. The depth dependence of the along isopycnal $\Delta NO_3/\Delta PO_4$ slopes observed by Quay and Wu (2015) illustrate a general trend that the impact of in situ OM degradation on dissolved nutrient concentrations in the ocean decreases with increasing depth as the OM flux and degradation rates decrease, water parcel ages increase and the impact of circulation and water mass mixing increase.

It is important to distinguish between the ratio of dissolved nutrient gradients, i.e., $\Delta NO_3/\Delta PO_4$, $\Delta DIC/\Delta PO_4$, $\Delta DIC/\Delta NO_3$ (where DIC = dissolved inorganic carbon) and the stoichiometric ratio of nutrient concentrations measured in a water parcel. The latter characteristic is a result of the all the inputs and losses of nutrients for a given water parcel (e.g., OM export, OM degradation, nitrogen fixation, denitrification, water mass mixing, CO_2 gas exchange, etc.). In contrast, the ratio of nutrient gradients represents the ratio of nutrient fluxes. For example, the ratio of the depth gradients of $\Delta NO_3/\Delta PO_4$ and $\Delta DIC/\Delta PO_4$ measured in the upper 300m of the water column represents the ratio of NO_3 to PO_4 and DIC to PO_4, respectively, being supplied to the surface layer from below by physical processes like turbulent

mixing, entrainment, upwelling, etc. There are significant differences between regional variations in the measured $\Delta NO_3/\Delta PO_4$ depth gradient ratio in the upper 300m of the Pacific Ocean and the NO_3/PO_4 concentration ratio of water parcels in the surface layer and at 250m (**Fig. 1**). The NO_3/PO_4 of water parcels ranges widely from 0 to 15 in the surface layer and from 6 to 15 at 250m with minima in the subtropics. In contrast, the range in $\Delta NO_3/\Delta PO_4$ in the upper 300m is significantly higher and narrower at 13 to 19 and much closer to the Redfield ratio at 16.

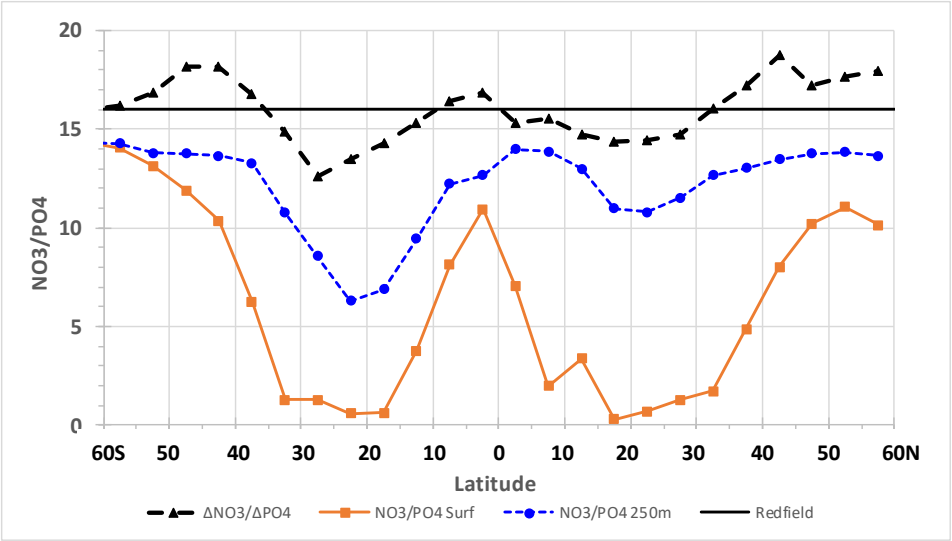

Fig 1. Regional trend in the ratio of the dissolved NO_3 to PO_4 concentration gradients ($\Delta NO_3/\Delta PO_4$) in the upper 300m compared to trends in the stoichiometric ratio of dissolved NO_3/PO_4 concentrations in water parcels from the surface layer and 250m along ~ 150°W in the Pacific Ocean and the Redfield ratio (16). Dissolved nutrient data (n=~5000) is from all GOSHIP P16 cruises based on GLODAP compilation (Olsen et al., 2016) and averaged on 5° latitude intervals.

There is a direct link between the ratio of nutrient fluxes ($\Delta DIC/\Delta NO_3/\Delta PO_4$) and the C/N/P of OM being exported. In the simplest situation where the vertical flux of dissolved nutrients at the base of the photic layer is the sole source of nutrient input to the photic layer and export of OM is the sole nutrient sink, then at steady-state the ratio of $\Delta DIC/\Delta NO_3/\Delta PO_4$ being supplied equals the C/N/P of the exported OM. Although nitrogen fixation and air-sea CO_2 exchange alter this simple situation, as discussed below, there is a clear dependence between the ratios of dissolved nutrients being supplied and organic nutrients being exported. Estimating the ratio of nutrient fluxes is significantly more robust than estimating the fluxes themselves because the flux ratio only depends on the measured concentration gradients but not an estimate of the rates of advection, turbulent mixing, entrainment, etc.

In this study, the first objective is to establish the link between the C/N/P of exported OM and the dissolved $\Delta DIC/\Delta NO_3/\Delta PO_4$ depth gradient ratio in the upper layer (300m) of the Pacific Ocean. The second objective is to demonstrate the means to estimate regional variations in the C/N/P of exported OM based on observed dissolved $\Delta DIC/\Delta NO_3/\Delta PO_4$. To accomplish these goals simple surface layer DIC, NO_3 and PO_4 budgets are used. We find regional trends in observed $\Delta DIC/\Delta NO_3/\Delta PO_4$ across the Pacific Ocean basin that yield systematic, but different, regional trends in the estimated C/N/P of exported OM. The highest C/N/P for exported OM are found in the subtropics and lowest ratios in the equatorial region that agree with available observed particle C/N/P. We find that three factors primarily control the regional variations in the $\Delta DIC/\Delta NO_3/\Delta PO_4$ in the upper 300m of the ocean, i.e., the C/N/P of OM exported out of photic layer and subsequently degraded, the fraction of exported organic nitrogen supported by nitrogen fixation and fraction of exported organic carbon supported by net air-sea CO_2 gas exchange flux. We extend this analysis approach to bioactive trace elements (TE) using the ratio of measured depth gradients of dissolved Cadmium (Cd) and PO_4 to estimate regional trend in the Cd/P of exported OM.

2. Methods

2.1 Data Sets and $\Delta DIC/\Delta NO_3/\Delta PO_4$ calculation

The ratio of dissolved DIC, NO_3, PO_4 depth gradients ($\Delta DIC/\Delta NO_3/\Delta PO_4$) was determined using data collected during several north-south cruises in the Pacific Ocean (P16 cruises occurred between ~70°S and 60°N along ~150°W) as part of the GOSHIP program and compiled by the GLODAP program (Key et al., 2015; Olsen et al., 2016). The nutrient data (n ~ 5000) was averaged over 25m depth intervals between 0 and 300m (12 layers) and over 5° latitude bands from 60°S to 60°N. The $\Delta DIC/\Delta NO_3/\Delta PO_4$ was determined using a linear regression of concentrations in the layers between the base of the mixed layer and 300m. Determining the $\Delta DIC/\Delta NO_3/\Delta PO_4$ for specific P16 cruises that occurred between 1991 and 2015 indicates that the regional trend in $\Delta DIC/\Delta NO_3/\Delta PO_4$ is reproducible over decadal time scales in the Pacific Ocean (**Fig. S1**) which illustrates, first, the robustness of this characteristic and, second, that the uptake of anthropogenic CO_2 has no significant effect on the $\Delta DIC/\Delta NO_3/\Delta PO_4$ for the water residence times in the upper 300m. The measured DIC depth gradient was corrected for $CaCO_3$ dissolution based on the observed alkalinity depth gradient.

147 The alkalinity correction was only significant poleward of 55°S and 35°N where it accounted for
148 10-20% of the DIC gradient in the upper 300m. It is assumed that the corrected dissolved
149 $\Delta DIC/\Delta PO_4$ and $\Delta DIC/\Delta NO_3$ represent the effect of OM export and degradation processes.
150 Unless otherwise stated, $\Delta NO_3/\Delta PO_4$, $\Delta DIC/\Delta PO_4$ and $\Delta DIC/\Delta NO_3$ represents the ratio of the
151 vertical nutrient gradients measured over the upper 300m of the water column.

152 Additionally, the ratio of horizontal concentration gradients of dissolved DIC, NO_3 and
153 PO_4 in the surface ocean was determined using gridded GLODAP data at 1° latitude by 3°
154 longitude resolution. The meridional and zonal horizontal surface layer nutrient gradients
155 $[\Delta DIC/\Delta NO_3/\Delta PO_4]_h$ were averaged between 180°W and 130°W and over 5° of latitude. The
156 horizontal surface $[\Delta DIC/\Delta PO_4]_h$ and $[\Delta DIC/\Delta NO_3]_h$ gradients are much more variable than
157 $[\Delta NO_3/\Delta PO_4]_h$ especially in the subtropics where the NO_3 and PO_4 concentrations are low, i.e.,
158 ~50% of the surface $[\Delta DIC/\Delta PO_4]_h$ values were either negative or >300 whereas <20% of the
159 surface $[\Delta NO_3/\Delta PO_4]_h$ values were either negative or >40. The higher variability of the surface
160 $[\Delta DIC/\Delta PO_4]_h$ and $[\Delta DIC/\Delta NO_3]_h$ gradients are in part a result of there being only half as much
161 DIC data as for NO_3 and PO_4 and the impact of air-sea CO_2 gas exchange on surface DIC
162 resulting from seasonal temperature variations (Takahashi et al., 2009).

163 Regional trends in the indirect estimates of the C/N/P of exported OM were compared to
164 observed trends in available particle C/N/P data from the Pacific Ocean (60°S to 50°N). The
165 primary source of particle data is the compilation by Martiny et al. (2014). We imposed a
166 constraint of a minimum particulate phosphorous (POP) concentration of 10 nM to eliminate
167 anomalously high N/P and C/P in the subtropical gyres. At the time-series Stn. ALOHA (23°N
168 153°W) this constraint reduced the mean C/P and N/P by 10% and simultaneously reduced the
169 variability (SD) by 30%. Particle data from coastal ocean sites were excluded from the Martiny
170 et al. compilation with the most notable sites being located in the California Current System and
171 on the Bering Sea shelf. The filtered data set had ~1700 measurements of C/P and N/P and
172 ~6200 measurements of C/N for suspended particles. The spatial coverage in C/P and N/P is
173 limited to 30°S to 40°N with about half of the observations (~760) occurring at the time series
174 station ALOHA whereas the C/N data set expanded coverage to 60°S to 50°N. Additionally,
175 updated C/N/P data was added for suspended particles in the upper 100m (n=190) and sediment
176 trap material at 150m (n=160) collected at Stn ALOHA between 2000 and 2018 and at Ocean

Station Papa (OSP, 50°N 145°W) between 1987 and 1996 (Wong et al., 1999) and suspended material collected in the upper 100m using an in situ filtration method (MULVFS) at Stn K2 (47°N 161°E) in the subpolar N. Pacific (Bishop and Wood, 2008). Particle C/P and N/P data from HOT and SUPERHI sites measured between 2002 and 2012 were corrected for a particulate phosphorous measurement method artifact (Fujeiki et al., 2015).

Dissolved cadmium (Cd) data measured on the GOSHIP P16 cruises in 2005-2006 (Landing et al., 2019) was used to determine the vertical $\Delta Cd/\Delta PO_4$ in the upper 300m.

2.2 Surface Layer Dissolved DIC, NO_3 and PO_4 Budgets

Surface layer nutrient budgets were used to link the C/N/P of exported OM and the observed gradient ratios of $\Delta DIC/\Delta NO_3/\Delta PO_4$ in the upper 300m. The budget terms included nutrient input from the physical supply (from advection, mixing, entrainment, eddies, etc.) and loss from exported OM which includes both particulate and dissolved OM. The NO_3 budget had an additional term representing inorganic nitrogen (N) input from N fixation. The DIC budget had an additional term representing air-sea CO_2 exchange which could be either a DIC source or sink. The expressions for these budgets are as follows.

$$Z*dPO_4/dt = - Export\_P + Supply\_PO_4 \quad (1)$$

$$Z* dNO_3/dt = - Export\_N + Supply\_NO_3 + N\ fixation\ rate \quad (2)$$

$$Z* dDIC/dt = - Export\_C + Supply\_DIC \pm Air\text{-}sea\ CO_2\ gas\ flux \quad (3)$$

where *t* is time, *Z* represents the surface layer depth, *Export* represents the export rate of OM and *Supply* represents the supply rate of dissolved nutrients by physical processes. It is assumed that *Export*_N = *Export*_P*$(N/P)_{OM}$, *Export*_C = *Export* P*$(C/P)_{OM}$, *Supply*_NO_3 = *Supply*_PO_4*$(\Delta NO_3/\Delta PO_4)$ and *Supply*_DIC = *Supply*_PO_4*$(\Delta DIC/\Delta PO_4)$.

The NO_3, PO_4 and DIC surface layer budgets can be used to estimate the C/N/P of the exported OM. At steady-state, the following relationships exist between ratio of dissolved nutrients being supplied ($\Delta NO_3/\Delta PO_4$, $\Delta DIC/\Delta PO_4$, $\Delta DIC/\Delta NO_3$) and the N/P, C/P and C/N of organic matter being exported.

$$(N/P)_{OM} = (\Delta NO_3/\Delta PO_4) / (1\text{-}Fn) \quad (4)$$

$$(C/P)_{OM} = (\Delta DIC/\Delta PO_4) / (1\text{-}Fc) \quad (5)$$

$$(C/N)_{OM} = (\Delta DIC/\Delta NO_3) \bullet (1\text{-}Fn) / (1\text{-}Fc) \quad (6)$$

Fn equals the fraction of OM exported nitrogen supplied by N fixation and Fc is the fraction of OM exported carbon supplied by CO_2 gas invasion (a negative value if CO_2 gas is evading from the surface ocean). It is assumed that all other dissolved nutrient inputs and losses to the surface layer are negligible compared to physical supply and OM export, respectively. Note that when the N fixation and CO_2 flux rates are zero then the estimated N/P, C/P and C/N of exported OM equals the observed supply ratio of $\Delta NO_3/\Delta PO_4$, $\Delta DIC/\Delta PO_4$ and $\Delta DIC/\Delta NO_3$, respectively.

Estimates of the regional trends in the N/P, C/P and C/N of exported OM were determined from surface layer budgets for DIC, NO_3 and PO_4 based on equations 4-6. The mean and standard deviation (SD) of the linear regression-based estimate of $\Delta NO_3/\Delta PO_4$, $\Delta DIC/\Delta PO_4$ and $\Delta DIC/\Delta NO_3$ in the upper 300m was determined for each 5° latitude band. A random value of $\Delta NO_3/\Delta PO_4$, $\Delta DIC/\Delta PO_4$ and $\Delta DIC/\Delta NO_3$ was chosen based on the mean and SD and an assumed normal distribution. A value for Fc and Fn was randomly chosen over possible range of 0 to 0.9 for each variable and then the N/P, C/P and C/N of export OM was calculated from equations 4-6, respectively. This procedure was repeated 10,000 times. A subset of solutions was selected that yielded N/P, C/P and C/N values within the ranges of 7 to 40, 40 to 270 and 5 to 14, respectively, which encompassed 95% (±2SD) of the ranges observed for particles in the Pacific Ocean (Martiny et al., 2013a and 2013b). A mean and standard deviation for N/P, C/P and C/N was calculated from the solution subset for each latitude band. Fn was assumed equal to zero when N* (=NO_3 - 16*PO_4 + 2.9) exceeded zero (Deutsch et al., 2001) which coincided with surface NO_3 concentration exceeding ~0.3 umol/kg in a latitude band. Although the possible range for Fn was 0 to 0.9 a maximum value of Fn ~ 0.6 was determined for the subset of solutions in all latitude bands where N fixation was allowed to occur which agrees well with inverse model results (Wang et al., 2019). Fc was assumed to vary between 0 and -0.9 between 10°S and 10°N as the equatorial Pacific is a region of CO_2 evasion (Takahashi et al., 2009).

The calculated C/N/P of exported OM is most sensitive to the observed $\Delta DIC/\Delta NO_3/\Delta PO_4$ with the N/P, C/P and C/N equaling the observed $\Delta NO_3/\Delta PO_4$, $\Delta DIC/\Delta PO_4$ and $\Delta DIC/\Delta NO_3$, respectively, when Fc and Fn equaled zero. For latitude bands where Fn and Fc exceeded zero then the N/P and C/P of the exported OM exceeded the $\Delta NO_3/\Delta PO_4$ and

234 $\Delta DIC/\Delta PO_4$ respectively. Contrastingly, in the equatorial ocean the calculated C/P and C/N of
235 exported OM was less than the $\Delta DIC/\Delta PO_4$ and $\Delta DIC/\Delta NO_3$, respectively, because of CO_2 gas
236 evasion. The imposed maximum and minimum limits of N/P, C/P and C/N further constrained
237 the subset of selected scenarios by essentially limiting the range in Fc and Fn. For example, if a
238 randomly picked value of Fc was 0.9 and the observed $\Delta DIC/\Delta PO_4$ was 100 then the calculated
239 C/P of exported OM for this scenario would equal 1000 and the imposed limit of 270 would
240 exclude this scenario from selection. The same limits on N/P, C/P and C/N of particles were
241 applied to all latitude intervals.

242 2.3 *Vertical and Horizontal $\Delta DIC/\Delta NO_3/\Delta PO_4$ and Nutrient supply*

243 The $\Delta DIC/\Delta NO_3/\Delta PO_4$ used to calculate the C/N/P of exported OM in equations 4-6
244 ideally represents all physical processes supplying nutrients to the surface layer, e.g. turbulent
245 mixing, upwelling, surface advection, eddies, etc. The relative importance of horizontal versus
246 vertical supply of nutrients to the photic layer of the ocean remains an open question. Letscher et
247 al. (2016) used output from a global biogeochemical model tuned to yield observed nutrient
248 distributions to indicated that one-third of the dissolved N and two-thirds of the dissolved P in
249 the surface layer of the subtropical N. Pacific are supplied by horizontal processes although the
250 circulation model was not eddy resolving. On the other hand, field observations based on
251 continuous float (Johnson et al., 2010) and seaglider (Nicholson et al., 2008) based O_2 and NO_3
252 data sets at Stn ALOHA indicate that vertical transport of NO_3 and O_2 by episodic isopycnal
253 uplift events associated with mesoscale eddies and Rossby waves are a primary mechanism
254 supplying nutrients to the photic layer in the subtropical ocean. Johnson et al. (2010) concluded
255 that episodic transport events could supply NO_3 to the photic layer at a sufficient rate (coupled
256 with N fixation) to support the observed OM export rate at Stn ALOHA and that within the water
257 column from the surface to 250m there is near equivalence between nutrient supply and demand.
258 In the subpolar N. Pacific at OSP Haskell et al. (2020) use multiyear (2009-2017) profiling float
259 and mooring based NO_3, pCO_2 and O_2 measurements to conclude that turbulent diffusion rates at
260 the base of the photic layer estimated from heat budgets at OSP (Cronin et al., 2015) supplied
261 sufficient NO_3 and DIC to support annual OM export. The increasing availability of continuous
262 T, S, NO_3, O_2 and pCO_2 measurements provided by floats, moorings and seagliders will
263 significantly improve estimates of turbulent mixing rates at the base of the photic layer (e.g.,

Cronin et al., 2015, Pelland et al., 2018), frequency of isopycnal displacement events (e.g., Nicholson et al., 2008; Johnson and Riser, 2010) and yield highly resolved vertical gradients of NO_3, DIC and O_2 in the upper ocean (e.g. Haskell et al., 2020) which together will help answer the question about importance of vertical versus horizontal nutrient supply in the surface ocean.

The key issue is how well the $\Delta DIC/\Delta NO_3/\Delta PO_4$ determined from depth gradients in the upper 300m represents all processes supplying dissolved inorganic nutrients to the surface layer. If the $\Delta DIC/\Delta NO_3/\Delta PO_4$ measured on depth gradients in the upper 300m is similar to the $\Delta DIC/\Delta NO_3/\Delta PO_4$ determined from horizontal concentration gradients in the surface layer, then both horizontal and vertical processes supplying nutrients will be accurately represented in equations 4-6. A comparison of nutrient gradient ratios focuses on $\Delta NO_3/\Delta PO_4$ because of the variability issues with surface $\Delta DIC/\Delta PO_4$ and $\Delta DIC/\Delta NO_3$ concentration gradients, discussed above. The vertical $[\Delta NO_3/\Delta PO_4]_z$ over the upper 300m is determined by averaging nutrient depth gradients measured during several P16 cruises over 5° latitude band (Fig. S1). The horizontal meridional and zonal concentration gradient ratios in the surface layer $[\Delta NO_3/\Delta PO_4]_h$ are determined from observed NO_3 and PO_4 concentrations based on the GLODAP data compilation (Olsen et al., 2016). A comparison between the observed $[\Delta NO_3/\Delta PO_4]_z$ and $[\Delta NO_3/\Delta PO_4]_h$ show clear regional trends (**Fig. 2**). One notable observation is that in the subpolar and equatorial oceans where there are significant surface PO_4 and NO_3 concentrations the $[\Delta NO_3/\Delta PO_4]_h$ at 16±4 is indistinguishable from $[\Delta NO_3/\Delta PO_4]_z$ at 17±1. This is important because it implies that $[\Delta NO_3/\Delta PO_4]_z$ should adequately represent both vertical and horizontal supplies of NO_3 and PO_4 to the surface layer in these regions. Another notable observation is that the horizontal surface transport of PO_4 (and NO_3) in the subtropics is near zero because of the very low concentrations of dissolved PO_4 (and NO_3) in the surface layer (**Fig. 2**). The horizontal advective PO_4 (and NO_3) transport in the surface layer was determined by multiplying meridional and zonal components of advective velocities based on ARGO (2001-2013 climatology) by the meridional and zonal PO_4 (and NO_3) gradients from GLODAP climatology and averaging zonally between 180°W and 130°W and over 5° latitude bands. The implication is that vertical supply of nutrients by turbulent mixing, upwelling, and eddy pumping (as discussed above) should dominate and be accurately represented by $[\Delta NO_3/\Delta PO_4]_z$ in the subtropics. That local vertical nutrient supply dominates over horizontal nutrient supply in the

subtropical Pacific Ocean agrees with the field-based studies at Stn. ALOHA but not the modeling results, discussed above.

Results and Discussion

3.1 Regional Trends in Dissolved ΔDIC/ΔNO₃/ΔPO₄ and C/N/P of Exported Organic Matter

There are clear regional trends in the dissolved $\Delta NO_3/\Delta PO_4$, $\Delta DIC/\Delta PO_4$ and $\Delta DIC/\Delta NO_3$ across the Pacific Ocean (**Fig. 3**). The $\Delta NO_3/\Delta PO_4$ has minima (~14) in the subtropics and maxima (~18) in subpolar regions. The $\Delta DIC/\Delta PO_4$ has minimum in the subtropical N. Pacific (~80) and a maximum in the subtropical S. Pacific (~180) as does $\Delta DIC/\Delta NO_3$ at ~5 and 12, respectively. There are clear regional trends in the budget-based estimates of the N/P, C/P and C/N of exported OM yet they are distinct from the $\Delta NO_3/\Delta PO_4$, $\Delta DIC/\Delta PO_4$ and $\Delta DIC/\Delta NO_3$ trends (**Fig. 3**). The estimated exported N/P ranges from ~16 to 22 with a minimum at the equator and maxima in the subtropics. Notably, the exported N/P significantly exceeds the $\Delta NO_3/\Delta PO_4$ in the subtropics but equals $\Delta NO_3/\Delta PO_4$ in the equatorial

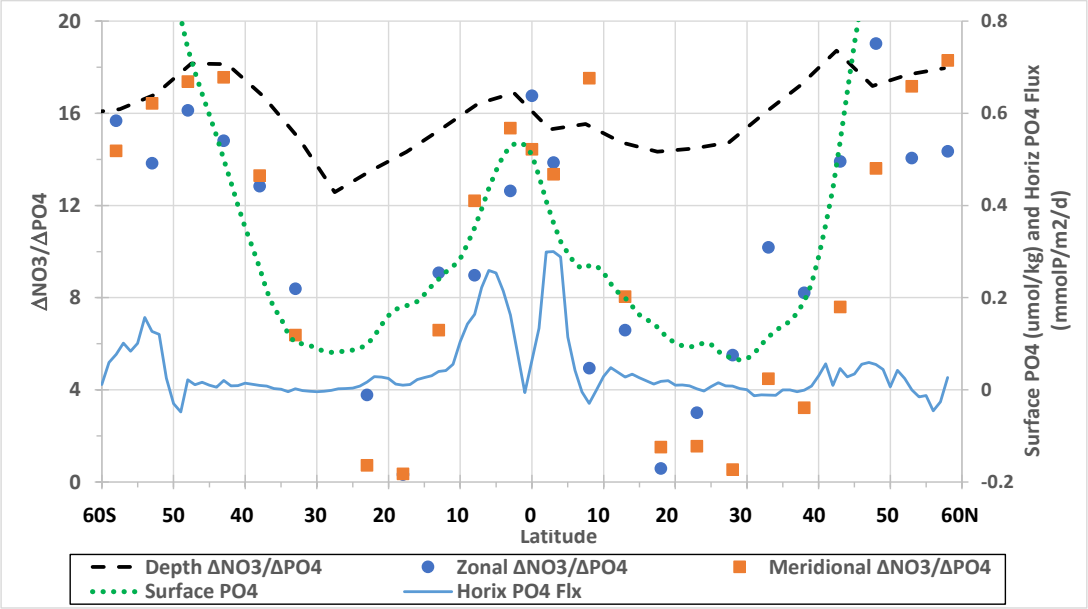

Figure 2. Regional trends in the mean observed vertical $[\Delta NO_3/\Delta PO_4]_z$ based on depth concentration gradients in the upper 300m and horizontal surface $[\Delta NO_3/\Delta PO_4]$ based on meridional and zonal surface nutrient concentration gradients using the GLODAP data compilation (Olsen et al., 2016) averaged between 170°W and 130°W and over 5° latitude intervals. Surface advective PO_4 flux (mmol P/m^2/d) is based on meridional and zonal surface PO_4 gradients and current velocities from a gridded ARGO data climatology.

and subpolar regions. The estimated exported C/P ranges from ~90 to 220 with maxima in the subtropical S. Pacific and a minimum in the equatorial region and exceeds the $\Delta DIC/\Delta PO_4$

everywhere except in the equatorial region. Similarly, the estimated exported C/N ranges from ~7 to 10 with maximum in the subtropical S. Pacific and a minimum in the equatorial region and exceeds the $\Delta DIC/\Delta NO_3$ poleward of ~30°. The estimated exported N/P, C/P and C/N exceed Redfield (106:16:1) everywhere except in the equatorial region.

The question arises why the budget-based estimates of exported N/P, C/P and C/N differ from the observed $\Delta NO_3/\Delta PO_4$, $\Delta DIC/\Delta PO_4$ and $\Delta DIC/\Delta NO_3$ of nutrients supplied to the surface layer, respectively. The simplest steady-state surface layer budget situation would be where the supply of dissolved nutrients by physical processes is exactly balanced by the loss of those nutrients in exported OM which would imply that the N/P, C/P and C/N of exported OM equals the $\Delta NO_3/\Delta PO_4$, $\Delta DIC/\Delta PO_4$ and $\Delta DIC/\Delta NO_3$ supplied, respectively. However, two processes alter this simple situation and can cause the C/N/P of exported OM to differ significantly from the $\Delta DIC/\Delta NO_3/\Delta PO_4$ supplied. First, nitrogen (N) fixation is a source of inorganic nitrogen. Second, air-sea CO_2 gas exchange can be either a source (invasion) or sink (evasion) of DIC. The occurrence of N fixation implies that the N/P of exported OM exceeds the $\Delta NO_3/\Delta PO_4$ being supplied at steady-state. Similarly, air-sea CO_2 invasion (evasion) implies that the C/P of exported OM is greater than (less than) the $\Delta DIC/\Delta PO_4$ being supplied. The quantitative relationships between $\Delta DIC/\Delta NO_3/\Delta PO_4$ being supplied, C/N/P of exported OM, N fixation and air-sea CO_2 exchange are shown in equations 4 - 6. For example, if N fixation supplied an amount of inorganic N equal to the NO_3 being supplied by physical processes, then the N/P of exported OM would be double the NO_3/PO_4 being supplied. Likewise, if air-sea CO_2 invasion contributed an equal amount of DIC as being supplied by physical processes then the C/P of exported OM would be double the DIC/PO_4 being supplied. To reiterate, the surface layer nutrient budgets assume any sources or sinks of inorganic nutrients other than those related to physical supply, N fixation and CO_2 gas flux are negligible in the upper 300m of the Pacific Ocean.

To be clear the C/N/P of the exported OM controls the $\Delta DIC/\Delta NO_3/\Delta PO_4$ being supplied, that is, the depth and horizontal surface gradient ratios for dissolved $\Delta DIC/\Delta NO_3/\Delta PO_4$ being supplied by physical processes adjust to the C/N/P of exported OM and the rates of OM export, N fixation and air-sea CO_2 exchange. The C/N/P of the plankton can vary substantially depending on the specific phytoplankton species, growth rates, growth limitations imposed by

availability of NO_3, PO_4, light, iron, etc., the abundances of macromolecules (proteins, lipids, carbohydrates) required to support photosynthesis rates and for energy or nutrient storage, etc. (e.g., Geider and La Roche, 2002; Agren, 2004; Klausmeier et al., 2004). The substantial variability of particle C/N/P in the surface ocean is illustrated by the five-fold range observed in C/P and N/P for suspended particles in the data set compiled by Martiny et al. (2014) and by the two-fold range in N/P (15-30) and C/P (100-200) measured on suspended particles in the surface layer at Stn. ALOHA over ~20 years (Fig. S2). The same overall mean C/N/P of 145/20/1 was observed by Martiny et al. and at Stn ALOHA (2000-2018) which is significantly greater than Redfield and underscores the point that the classical Redfield ratio does not represent an optimal C/N/P of phytoplankton but an average composition. Because the C/N/P of plankton varies substantially it is difficult to characterize the annual mean C/N/P of particles based on short-term direct measurements especially in regions with strong seasonality in primary production rates, nutrient availability, phytoplankton species, etc. A further complication is the role of exported dissolved organic matter (DOM) which on average contributes about 20% of the exported OM (Hansell et al., 2007). Because the DOM pool has both refractory and labile components the C/N/P of the exported and subsequently degraded labile DOM in the upper 300m can differ significantly from the C/N/P of bulk DOM in the surface layer (Hopkinson and Vallino, 2005). Hopkinson and Vallino measured the C/N/P of the labile component of the DOM at three coastal sites and at Stn ALOHA and found a consistent C/N/P of 199/20/1. A model-based study of the C/N/P of labile DOM yielded a similar value of 225/19/1 for labile DOM needed to best match the observed DOM distribution in the ocean (Letscher et al., 2015). If these results are representative ocean-wide then the impact of labile DOM export on the C/N/P of exported OM would be greatest in the subpolar and equatorial regions where the C/N/P of labile DOM differs most from the C/N/P of the particles and least in the subtropical gyres where the C/N/P of labile DOM is similar to the C/N/P of particles (**Fig. 3**), as discussed below.

There are several advantages of estimating the C/N/P for exported OM based on the observed dissolved gradient ratio of $\Delta DIC/\Delta NO_3/\Delta PO_4$ in the upper ocean. The $\Delta DIC/\Delta NO_3/\Delta PO_4$ integrate over the ventilation time of these shallow waters (a few years) and thus provide longer term estimates of the C/N/P of exported OM which avoids the problem of temporal variability in direct measurements of the C/N/P of OM. The estimate of exported C/N/P represent all processes that export OM (e.g., particle sinking, transport of DOM, diel migration of

zooplankton, etc.) and avoids the issue of whether the measured C/N/P of suspended particles accurately represents the C/N/P of exported OM. The budget-based method relies directly on observations and doesn't require biogeochemical model output which avoids possible model biases. Because high quality dissolved nutrient data is available on global scales through the GOSHIP program the C/N/P of exported OM potentially can be indirectly estimated across all ocean basins. Lastly, the same approach can be applied to bioactive trace elements being measured by the GEOTRACES program to estimate the TE/C/N/P of exported OM, as illustrated below.

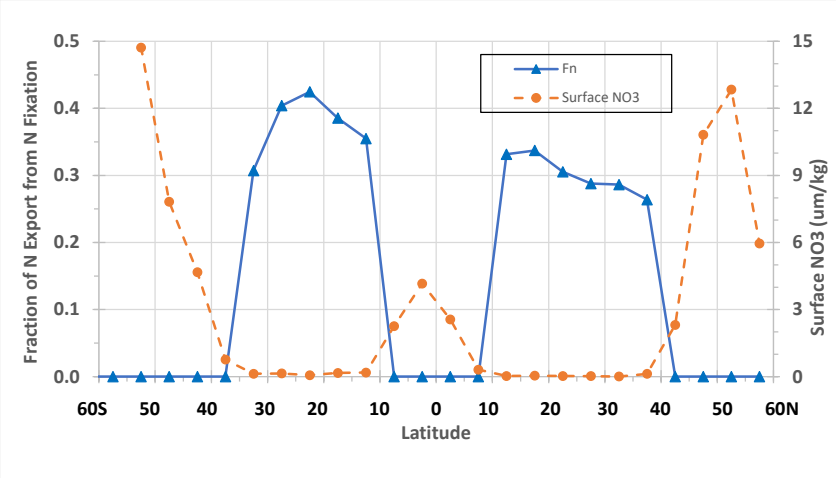

Figure 4. Regional trend in the fraction of exported organic nitrogen supported by nitrogen fixation determined from the NO_3 budget (Fn in eq. 4) and nitrate concentration in surface layer along ~150°W in the Pacific Ocean.

3.2 Impact of N fixation and Air-Sea CO_2 Exchange on $\Delta DIC/\Delta NO_3/\Delta PO_4$

N fixation in the subtropics causes the N/P of exported OM to exceed the $\Delta NO_3/\Delta PO_4$ being supplied. At Stn. ALOHA in the subtropical N. Pacific Karl et al. (1997) determined that N fixation contributed 32-48% of exported organic N based on a NO_3 budget approach and the $\delta^{15}N$ of exported particles. Using nutrient depth profiles measured monthly at Stn ALOHA between 2010 and 2018 yields an observed $\Delta NO_3/\Delta PO_4$ of 14.2±1.7 measured over 300m which when combined with the measured N/P of 21±5 for suspended particles and 24±8 sediment trap during the same time interval indicate that N fixation would support 33-43% of the exported organic N in good agreement with the Karl et al estimate. Combining the budget based estimated Fn of 0.38±0.11 and 0.30±0.08 for the subtropical S. and N. Pacific (**Fig. 4**),

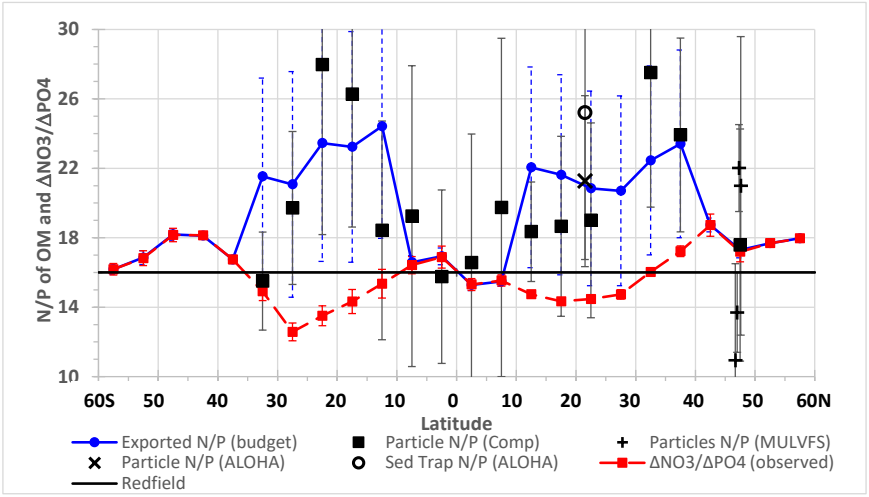

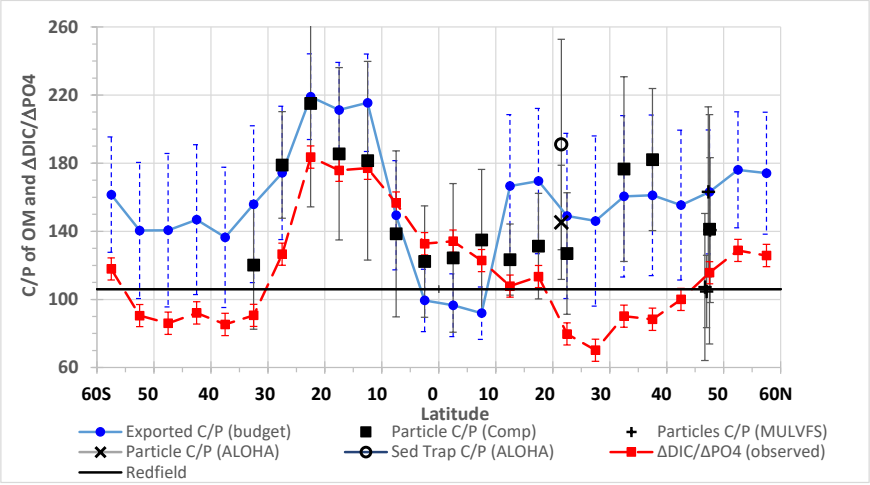

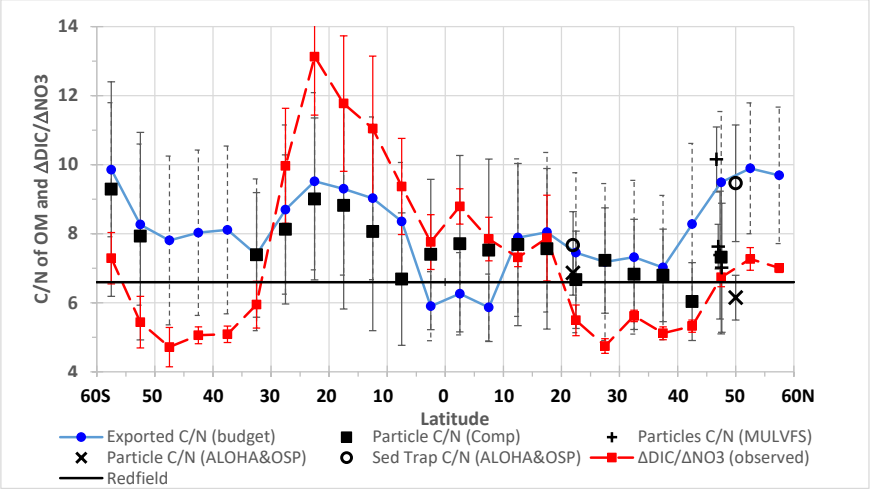

Figure 3. Regional trends in the observed $\Delta NO_3/\Delta PO_4$ (top), $\Delta DIC/\Delta PO_4$ (middle) and $\Delta DIC/\Delta NO_3$ (bottom) measured in the upper 300m, budget-based estimates of N/P, C/P and C/N for exported organic matter and observed N/P, C/P and C/N for particles. Error bars represent ±1 SD of mean values averaged over 5° latitude bands. Particle data from global compilation (Martiny et al., 2014), samples collected at Stn K2 (Bishop and Wood, 2008) and multiyear samples collected at ALOHA and OSP (Wang et al., 1999).

388

respectively, with observed OM export rates of ~1 and 2.5 mols C/m^2/yr, respectively, for these regions (Quay et al., 2020) and an average C/N of 8.0 for exported OM (**Fig. 3**) yields an estimated total N fixation rate of 79±38 Tg N/yr for the Pacific Ocean which lies midway between the independent estimates of 59±14 Tg/yr based on observed denitrification rate and NO_3 depth distributions (Deutsch et al., 2001) and inverse model estimates of 101±30 Tg/yr (Wang et al., 2019).

In all regions of the Pacific, except near the equator, the estimated exported C/P significantly exceeds the $\Delta DIC/\Delta PO_4$ whereas near the equator the estimated C/P is lower than

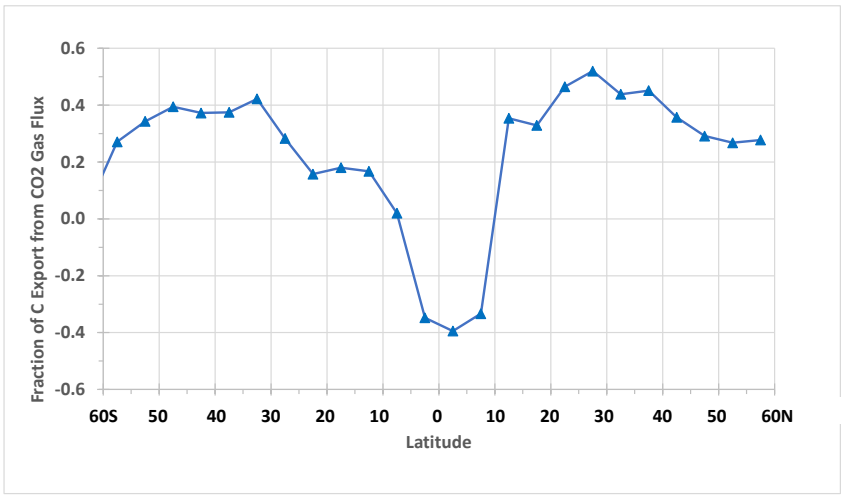

Figure 5. Regional trends in the fraction of organic carbon export supported by air-sea CO_2 flux (Fc in eq. 5). A negative value occurs when there is net CO_2 gas evasion from the surface ocean.

$\Delta DIC/\Delta PO_4$ (**Fig. 3**). This regional trend is a result of air-sea CO_2 gas invasion. Net CO_2 gas invasion is observed for most regions of the Pacific Ocean except the equatorial region where net CO_2 gas evasion is observed (Takahashi et al., 2009). The budget approach expresses air-sea CO_2 flux as a fraction of the exported organic C (Fc in eq. 5) and estimates of Fc are obtained from the budget scenarios that yield the observed $\Delta DIC/\Delta NO_3/\Delta PO_4$ each latitude band, as discussed above. There is a clear region trend in Fc with maxima in the subtropics at ~0.4 and minima in the equatorial region at ~ -0.3 (**Fig. 5**). In the subtropical N. Pacific, where the estimated C/P of exported OM at 160±42 exceeds the $\Delta DIC/\Delta PO_4$ being supplied at 91±6 and requires a Fc of 0.43±0.11 which compares well to previous independent Fc estimates of 0.31-0.43 at Stn ALOHA based on multi-year DIC budgets (Quay et al., 2003; Keeling et al., 2004). In the equatorial region, in contrast to the subtropics, the observed $\Delta DIC/\Delta PO_4$ at 134±8 being

supplied is greater than the estimated exported C/P at 109±21 which is a result of air-sea CO_2 evasion and requires an Fc of -0.26±0.06. The regional trends in exported C/N and $\Delta DIC/\Delta NO_3$ have similar patterns to those for C/P and $\Delta DIC/\Delta PO_4$ except in the subtropical S. Pacific, where the estimated exported C/N is less the $\Delta DIC/\Delta NO_3$ being supplied. In this region, the relative impact of N fixation on N/P export (Fn=0.38) exceeds the relative impact of CO_2 invasion on C/P export (Fc=0.24) which causes the $\Delta DIC/\Delta NO_3$ being supplied to exceed the C/N of exported OM (see eq. 6).

3.3 Comparison Between Budget Estimated and Observed C/N/P of Particles

Overall, the regional trend in the estimated N/P, C/P and C/N of exported OM agrees with the available observed particle C/N/P which show subtropical maxima and an equatorial minimum (**Fig. 3**). The estimated exported N/P and observed particle N/P have subtropical peaks at 22±6 and 21±4, respectively, that are primarily a result of the high N/P at 20-35 for cyanobacteria including diazotrophs (Martiny et al., 2013; Letelier and Karl, 1998) and at 20 for labile DOM (Hopkinson and Vallina, 2005). The estimated exported N/P and observed particle N/P have equatorial minima at 16±1 and 17±5, respectively. A similar subtropical maximum and equatorial minimum for the N/P of exported OM was determined by Weber and Deutsch (2010) based on model calculations which showed that high N/P (~20) in subtropics and low values in equatorial (~16) and subpolar regions (~10) yielded a better match to observed NO_3 distribution in ocean than a constant N/P at Redfield. The inverse relationship between estimated N/P and surface NO_3 concentration is expected based on the theory that phytoplankton should exhibit low N/P under optimal growth conditions and high N/P under limited growth conditions (Klausmeier et al., 2004) and observations of Geider and La Roche (2002) that phytoplankton exhibited the lowest N/P in nutrient replete conditions and highest N/P under oligotrophic nutrient deficient conditions.

The estimated exported and observed particle C/P and C/N have maxima in the subtropics and a minimum in the equatorial region (**Fig. 3**). In the subtropics, the estimated exported C/P at 177±40 agrees with the observed particle C/P at 157±40 as does the C/N for estimated exported OM at 8.2±2.4 and observed particles at 7.6±1.9. The high C/N/P for particles and exported OM is likely a result of the dominance of cyanobacteria in these nutrient depleted subtropical regions. Martiny et al. (2013) measured a C/N/P for *Prochlorococcus* at

235/35/1 and *Synechococcus* at 161/25/1 and Letelier and Karl (1998) measured a C/N/P at 271/42/1 for *Trichodesmium.* Similarly, the mean C/P of 145(±33)/21(±5)/1 is measured for suspended particles (<100m) at Stn ALOHA (2000-2018) where *Prochlorococcus* dominates (Campbell and Vaulett, 1993). It is worth noting that the C/N/P of material collected in sediment traps at ~150m at Stn ALOHA (2000-2018) at 190(±62)/25(±8)/1 is significantly higher than the C/P of suspended particles. This observation raises the question of how well the elemental composition of suspended particles in the photic layer represents exported particles. A C/N/P of 154/18/1 was measured for labile DOM in the surface layer at Stn ALOHA (Hopkinson and Vallino, 2005). In the equatorial region the estimated exported C/N/P of 109(±21)/16(±1)/1 is and observed C/N/P for particles at 126(±36)/17(±5)/1 are significantly lower than in the subtropical gyres, closer to the Redfield ratio and likely a result of increased contribution to exported OM by eukaryotes for which Martiny et al. (2013) measured a C/N/P of 107/16/1.

The largest discrepancy between budget-based C/N/P of exported OM and observed C/N/P of suspended particles possibly occurs in the subpolar N. and S. Pacific. Unfortunately, there are no particle C/P or N/P data for the nutrient replete subpolar S. Pacific (south of 40°S) and all the particle data north of 40°N is from the Bering Sea shelf region (<100m) based on the data compiled by Martiny et al. (2014). Studies in the Gulf of Alaska have shown clear differences in phytoplankton community structure, growth rate, cell size and species composition between on- and off- shelf regions that are consistent with a gradient in iron availability (e.g., Strom et al., 2006). For this reason the particle data from the Bering Sea shelf region, where the mean C/N/P is 86/11/1, may not be representative of the particle C/N/P in the subpolar Pacific Ocean south of the Aleutian Islands where the budget based C/N/P of exported OM was estimated and iron limitation of productivity is important (Harrison et al., 1999). However, there are a few possible factors to explain why the C/N/P of exported OM would be significantly greater than the C/N/P of suspended particles in the subpolar N. Pacific. First, the C/N/P of the exported particles may be different from the suspended particles as Wong et al. (1999) observed at OSP (50°N 145°W) where the C/N of organic material collected in sediment traps (150-200m) at 9.5 was significantly higher than the C/N measured on suspended particles in the surface layer at 6.2 based on data collected over multiple years. Second, exported DOM could significantly increase the C/N/P of exported OM as Hopkinson and Vallini (2005) measured a consistent C/N/P of 199/20/1 for labile DOM at both coastal and oligotrophic sites. In nutrient replete

regions where fast sinking diatoms or coccolithophores are a significant component of the exported particles the impact of their degradation on the $\Delta DIC/\Delta NO_3/\Delta PO_4$ in the upper 300m would be reduced. In this situation, the export and degradation of labile DOM in the upper 300m would be more important and shift the observed $\Delta DIC/\Delta NO_3/\Delta PO_4$ towards 199/20/1. Haskell et al. (2020) came to a similar conclusion at OSP, based on multiyear (2009-2017) float and mooring based photic layer NO_3 and DIC budgets, that an observed decrease in the C/N of exported OM with increasing depth was likely the result of a shift from DOM to particle degradation. Haskell et al. estimated that a C/N of 8.8±3.5 for exported OM from the photic layer was needed to explain the observed annual cycles of DIC and NO_3 at OSP which significantly exceeded the C/N of 5.5±0.2 measured for suspended particles at OSP.

The situation in the subpolar S. Pacific is different from the subpolar N. Pacific. The estimated mean exported C/N/P at 145/17/1 south of 40°S (**Fig. 3**) is significantly greater than the C/N/P for particles of 73/13/1 collected in the subpolar (40°-60°S) Indian Ocean (Martiny et al., 2014). Although the explanations for the difference between estimated and observed C/N/P discussed above for the subpolar N. Pacific could apply in the subpolar S. Pacific there is an alternative explanation that seems more likely. If the majority of nutrients supplied vertically in the subpolar S. Pacific are not consumed by OM export but are removed by surface advection of dissolved nutrients, then the C/N/P of exported OM would be poorly constrained by the observed $\Delta DIC/\Delta NO_3/\Delta PO_4$. Support for this explanation comes from the magnitude of estimated horizontal advective transport of dissolved NO_3 in the surface layer in the subpolar S. Pacific (mainly equatorward) which at 3.0±0.4 mmol $N/m^2/d$ represents a ~4x greater loss than the organic N export rate estimated at ~ 0.8±0.3 mmol $N/m^2/d$ in this region (Arteaga et al., 2019). In this situation the budget approach applied here would not yield useful estimates of the C/N/P of exported OM because the impact of the C/N/P of exported OM would have only a minor effect on the vertical (and horizontal) $\Delta DIC/\Delta NO_3/\Delta PO_4$ gradient ratio. Thus, the subpolar S. Pacific appears to be a region where the observed dissolved nutrient distributions (even in the upper 300m) are minimally affected by degradation of OM matter exported locally and instead are largely controlled by external processes, i.e., nutrient composition of upwelling water. The situation in the subpolar N. Pacific is different because of the horizontal surface advective flux of NO_3 at 0.1±1.1 mmol $N/m^2/d$ is lower than the estimates of OM export at ~0.6±0.2 mmol $N/m^2/d$ (Haskell et al., 2020). Thus, in the subpolar N. Pacific the dominant nutrient loss term should be

OM export and the budget-based method should provide useful estimates of C/N/P. A difference between the estimated C/N/P of exported OM and observed particle C/N/P in the subpolar N. Pacific would require other explanations, as discussed above.

3.4 Variability in C/N/P of the ocean's biological pump

The appropriate C/N/P to describe the ocean's biological pump depends on the depth horizon of interest. If one is interested in the OM being exported at the base of the photic or mixed layer then there are large regional variations in the C/N/P. A consistent result in the subtropical Pacific Ocean is that the C/N/P of exported OM based on nutrient budgets (mean of 177/22/1) and observed suspended particles (mean of 157/21/1; Martiny et al., 2014) significantly exceed Redfield (106/16/1) (**Fig. 3**). The likely reasons are the dominance of cyanobacteria and diazotrophs in these regions of the Pacific Ocean with both species having high C/N/P in the 160/25/1 to 240/40/1 range (e.g., Martiny et al., 2013; Letelier and Karl, 1998) and the contribution by exported labile DOM with a C/N/P of ~200/20/1 (Hopkinson and Vallini, 2005). In the equatorial Pacific the estimated C/N/P of exported OM at 109/16/1 and observed particle C/N/P at 126/17/1 is significantly lower than in the subtropics and closer to Redfield. In nutrient replete regions a higher proportion of the phytoplankton pool is comprised of eukaryotes with a lower C/N/P of ~ 107/16/1 (Martiny et al., 2013).

As the depth horizon of interest gets deeper the regional variations in the C/N/P of the biological pump decrease for a couple of reasons. First, the contribution of small phytoplankton with slow sinking rates and labile DOM with short turnover times and high C/N/P to the degrading pool of OM decreases with depth whereas the contribution of larger and faster sinking particles with lower C/N/P increases. This trend increases the weighting of the C/N/P of OM being degraded to nutrient replete regions where larger phytoplankton were exported as depth increases. This effect was observed during VERTEX where at the subtropical Stn. ALOHA ~75% of the particles were degraded in the upper 300m whereas at subpolar Stn. K2 this fraction decreased to 50% (Martin et al., 1987). Similarly, inverse model results indicate that the fraction of surface particle flux present at 1500m is 3-4x greater in the subpolar regions compared to subtropical regions with the primary controlling factor being particle size (Weber et al., 2016). Second, the effects of water mass mixing increase with depth as water parcels ages increase. Along isopycnal mixing integrates regional variations in C/N/P of exported OM on the dissolved

nutrient distribution and expands the spatial extent of the impact of degradation of OM exported from nutrient replete (equatorial and subpolar) regions across the main thermocline of the ocean. In this sense, the Redfield ratio yields a large phytoplankton and nutrient replete regionally biased view of the ocean's biological pump which represents the exported OM reaching the main thermocline (500-1500m) but does not accurately represent the C/N/P of OM being exported from the photic layer. The shallow recycling of OM with high C/N/P has a potentially important impact on CO_2 sequestration. Although a high C/N/P of exported OM increases the efficiency of carbon sequestration, the shallow degradation of this OM (<300m) and short ventilation times of this surface layer would significantly shorten the time scale of the CO_2 sequestration gain.

3.5 Applying the Budget Approach to Trace Element Composition of Exported OM

To evaluate whether the principle of a budget-based approach could be used to establish the link between the bioactive trace element composition (TE/C/N/P) of exported organic matter and the dissolved trace element gradients in the upper ocean it was applied to Cadmium (Cd). The ratio of dissolved Cd to PO_4 depth gradients in the upper 300m ($\Delta Cd/\Delta PO_4$) was determined based on dissolved Cd and PO_4 measurements during GOSHIP P16 cruises in 2005/6 (70°S to 60°N along ~150°W) in the Pacific Ocean (Landing et al., 2019). The vertical dissolved $\Delta Cd/\Delta PO_4$ is assumed to represent the physical supply ratio to the photic layer analogous to $\Delta DIC/\Delta NO_3/\Delta PO_4$. If there were no other significant sources of Cd or PO_4 to the surface ocean (e.g., atmospheric deposition) and exported OM was the only sink for dissolved Cd and PO_4 then the Cd/P of exported OM would equal the $\Delta Cd/\Delta PO_4$ being supplied at steady-state, i.e, analogous to the situation where the estimated N/P of exported OM equals the dissolved $\Delta NO_3/\Delta PO_4$ being supplied when Fn=0 (see eq. 4). There are clear regional trends in the dissolved $\Delta Cd/\Delta PO_4$ with subtropical minima and equatorial and subpolar maxima (**Fig. 6**) that are similar to the trends observed previously (Quay et al., 2015). Assuming any external sources of Cd and PO_4 are negligible in the upper 300m then the meridional trend in dissolved $\Delta Cd/\Delta PO_4$ represents the trend in Cd/P of exported OM and this trend can be compared to the observed Cd/P of particles measured in the photic layer using samples collected by the MULVFS method at a few sites in the Pacific Ocean (Bourne et al., 2018). The observed particle Cd/P shows a subtropical minima and equatorial and subpolar maxima similar to the estimated Cd/P of exported OM trend with values that agree well in the subtropics. The higher particle Cd/P

observed in nutrient replete regions has been previously reported and attributed to several mechanisms (e.g., species composition, Fe limitation, phytoplankton growth rate, Zn availability, etc., see Bourne et al., 2018). However, the observed particle Cd/P data are significantly higher than the budget-based estimated Cd/P of exported OM in the nutrient replete regions. There is a tendency for the large particles (>51µm) to have lower Cd/P which agrees better with the dissolved $\Delta Cd/\Delta PO_4$ and raises the question of how well the Cd/P of total suspended particles represents the Cd/P of exported organic matter. One explanation of the difference in Cd/P for suspended particles versus exported OM would require preferential recycling between particulate and dissolved Cd compare to phosphorous within the euphotic zone. Another possible factor is

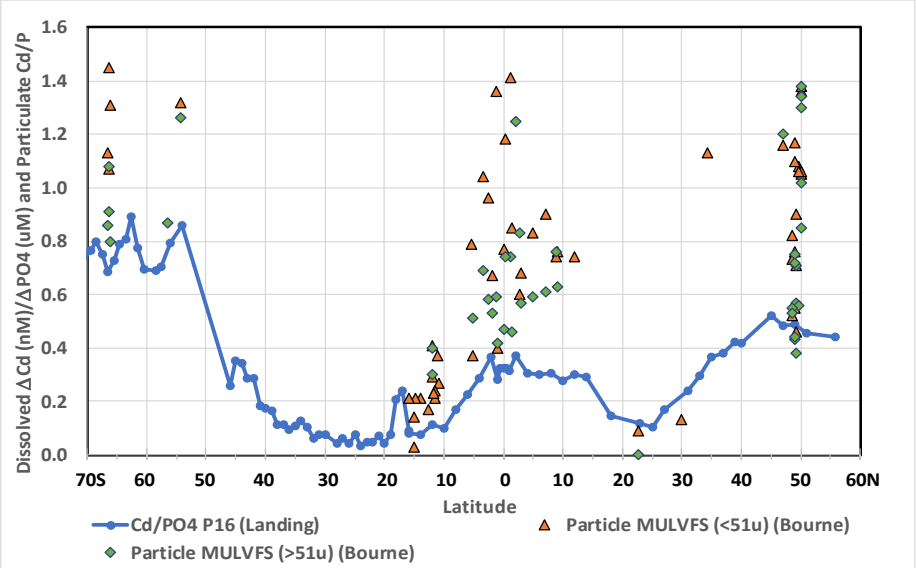

Figure 6. Regional trends in the dissolved $\Delta Cd/\Delta PO_4$ depth gradient ratio (nM/µM) in upper 300m based on measurements during GOSHIPS P16 cruises along 150°W (2005-06) by Landing et al. (2019) and measured Cd/P (nmol/µmol) of particles (<51µ and >51µ size classes) in upper 100m collected by the MULVFS method in the Pacific Ocean (Bourne et al., 2018).

the potential impact of exported DOM which could contribute to a difference between the Cd/P of exported OM and suspended particles. It is worth reiterating that estimating the TE/P of exported OM from the observed dissolved $\Delta TE/\Delta PO_4$, as done here for Cd/P, has the advantage of providing a multi-year estimates and avoiding the issue of temporal variability in particulate TE/P which makes it difficult to use single cruise measurements of particulate TE/P to accurately represent the mean value for a region. Additionally, for bioactive TEs that can have external inputs to the surface ocean then a significant difference between measured TE/P of exported OM and supplied $\Delta TE/\Delta PO_4$ could be used to constrain the magnitude of the external inputs.

3. Conclusions

The scarcity of measurements of the elemental composition of exported organic matter from the surface ocean yields a substantial gap in a fundamental characteristic of the ocean's biological pump and our understanding of how the dissolved nutrient and trace element distributions in the upper ocean are impacted by organic matter export and degradation. Here a new approach based on surface layer DIC, NO_3 and PO_4 budgets was used to establish the link the C/N/P of organic matter being exported and degraded and the measured distributions of dissolved nutrients in the upper 300m of the Pacific Ocean. The nutrient budgets provide a means to estimate the C/N/P of exported organic matter indirectly based on the ratio of measured gradients of dissolved nutrients which potentially could overcome the lack of measured organic matter composition data. The surface layer nutrient budgets indicate that three primary factors controlling regional variations in the dissolved DIC, NO_3 and PO_4 distributions in the upper layer of the ocean, that is, the C/N/P of exported organic matter, presence of nitrogen fixation and air-sea CO_2 gas exchange. Using the same approach, a surface layer budget for the bioactive trace element Cd was used to estimate regional trends in the Cd/P of exported OM based on the trends in the ratio of measured dissolved Cd and PO_4 depth gradients in the upper layer of ocean.

The generally good agreement between the regional variations in budget-based estimates of the C/N/P for exported OM and available particle C/N/P measurements in the Pacific Ocean encourages application of the method to other ocean basins using the availability of high-quality nutrient and trace element data provided by the GOSHIP and GEOTRACES programs. The observed regional trends in the dissolved $\Delta TE/\Delta DIC/\Delta NO_3/\Delta PO_4$ in the upper ocean should be a useful metric for evaluating the parameterization of organic matter export and degradation in ocean biogeochemical models. The observation-based results presented here for the Pacific Ocean support the findings of several modeling studies and underscore the importance of regional variability in the C/N/P of exported OM as a fundamental characteristic of the ocean's biological pump that has a major impact on regional variations in the dissolved nutrient distributions in the upper ocean.

606 *Acknowledgements and Data Availability*: The effort put into the GLODAP data compilation by
607 Bob Key and his colleagues is particularly appreciated. Particle and sediment trap elemental
608 data and depth profiles of dissolved nutrient for Stn. ALOHA were obtained via the Hawaii
609 Ocean Time-series HOT-DOGS application (University of Hawai'i at Mānoa and National
610 Science Foundation Award # 1756517). Bill Landing kindly allowed use of his dissolved Cd
611 data from P16. The work has been supported by the National Science Foundation as part of the
612 GEOTRACES program (OCE-1829796).

613 GLODAP data and their documentation are available at the Carbon Dioxide Information
614 Analysis Center (https://www.glodap.info/.). The particle composition data compiled by Martiny
615 et al. (2014) is found at https://datadryad.org/stash/dataset/doi:10.5061/dryad.d702p. Particle,
616 sediment trap and dissolved nutrient data for Stn ALOHA are found at
617 https://hahana.soest.hawaii.edu/hot/hot-dogs/interface.html. ARGO based surface current
618 velocities are found at
619 http://apdrc.soest.hawaii.edu/projects/Argo/data/statistics/Velocities/Ensemble_mean/1x1/m00/index
620 .html. The dissolved Cd data from P16 (Landing et al. 2019) is found at BCO-DMO archive at
621 https://www.bco-dmo.org/dataset/778403/data.

622

623

References

Agren, G.I. (2004). The C:N:P stoichiometry of autotrophs- theory and observations. *Ecological Letters,* 7, 185-191.

Arteaga, L. A., Pahlow, M., Bushinsky, S. M., & Sarmiento, J. L. (2019). Nutrient controls on export production in the Southern Ocean. *Global Biogeochemical Cycles*, *33*, 942–956. https://doi.org/10.1029/ 2019GB006236.

Ayers, J. M., & Lozier, M. S. (2012). Unraveling dynamical controls on the North Pacific carbon sink. *Journal of Geophysical Research*, *117*, C01017. https://doi.org/10.1029/2011JC007368

Bishop, J. K. B., & Wood, T. J. (2008). Particulate matter chemistry and dynamics in the twilight zone at VERTIGO ALOHA and K2 sites. *Deep-Sea Research, I*, 55, 1684–1706. https://doi.org/10.1016/j.dsr.2008.07.012

Bourne, H. L., Bishop, J. K. B., Lam, P. J., & Ohnemus, D. C. (2018). Global spatial and temporal variation of Cd:P in euphotic zone particulates. *Global Biogeochemical Cycles*, 32, 1123–1141. https://doi.org/10.1029/2017GB005842

Bushinsky, S. M., & Emerson, S. R. (2018). Biological and physical controls on the oxygen cycle in the Kuroshio Extension from an array of profiling floats. *Deep Sea Research I*, *141*, 51–70. https://doi.org/10.1016/j.dsr.2018.09.005

Campbell, L. & Vaulot, D. (1993). Photosynthetic picoplankton community structure in the subtropical North Pacific Ocean near Hawaii (station ALOHA). *Deep-Sea Research I*, 40, 2043-2060.

Cronin, M. F., Pelland, N. A., Emerson, S. R., & Crawford, W. R. (2015). Estimating diffusivity from the mixed layer heat and salt balances in the North Pacific. *Journal of Geophysical Research: Oceans*, *120*, 7346–7362. https://doi.org/10.1002/2015JC011010

Deutsch C., Gruber N., Key, R.M., Sarmiento J.L., & Ganachaud, A. (2001). Denitrification and N_2 fixation in the Pacific Ocean. *Global Biogeochemical Cycles,* 15, 483–506.

Fassbender, A. J., Sabine, C. L., & Cronin, M. F. (2016). Net community production and calcification from 7 years of NOAA Station Papa Mooring measurements. *Global Biogeochemical Cycles* 30: 250–267.

Fujeiki, L. A., Santiago-Mandujano, F., Fumar, C., Lukas, R., & Church, M. (2015). *Hawaii Ocean Time-series Data Report 24: 2012*.

Geider, R.J.. & LaRoche, J. (2002). Redfield revisited: Variability of C:N:P in marine microalgae and its biochemical basis. *European Journal of Phycology*, 37, 1-17.

Gray, A., Johnson, K. S., Bushinsky, S. M., Riser, S. C., Russell, J. L., Talley, L. D., Wanninkhof, R., Williams, N.L., & Sarmiento, J.L. (2018). Autonomous biogeochemical floats

667 detect significant carbon dioxide outgassing in the high-latitude Southern Ocean. *Geophysical*
668 *Research Letters*, *45*, 9049–9057, https://doi.org/10.1029/2018GL078013
669
670 Hansell, D.A., Carlson, C.A., Repeta, D. J. & Schlitzer, R. (2007). Dissolved organic matter in
671 the ocean: a controversy stimulates new insights, *Oceanography*, 22, 206-211.
672 Harrison, P.J., Boyd, P.W., Varela, D.E., Takeda, S., Shiomoto, A., & Odate, T. (1999).
673 Comparison of factors controlling phytoplankton productivity in the NE and NW subarctic
674 Pacific gyres. *Progress in Oceanography*, 43, 205-234.
675
676 Haskell, W. Z. II, Fassbender, A. J., Long, J. S., & Plant, J. N. (2020). Annual net community
677 production of particulate and dissolved organic carbon from a decade of biogeochemical
678 profiling float observations in the Northeast Pacific. *Global Biogeochemical Cycles*, *34*,
679 e2020GB006599, https://doi.org/10.1029/2020GB006599.
680
681 Hopkinson, C.S., & Vallino, J.J. (2005) Efficient export of carbon to the deep ocean through
682 dissolved organic matter. *Nature,* 433, 142-145.
683
684 Johnson, K. S., Riser, S. C., & Karl, D. M. (2010). Nitrate supply from deep to near-surface
685 waters of the North Pacific subtropical gyre. *Nature*, *465*, 1062–1065.
686 https://doi.org/10.1038/nature09170
687
688 Karl D.M., Letelier, R., Tupas, L., Dore, J., Christian, J., & Hebel, D. (1997). The role of
689 nitrogen fixation in biogeochemical cycling in the subtropical North Pacific Ocean. *Nature,* 388,
690 533-538.
691
692 Karl D.M., Bjorkman, K.M., Dore, J.E., Fujieki, L., Hebel, D.V., Houlihan, T., Letelier, R.M., &
693 Tupas, L.M. (2001). Ecological nitrogen-to-phosphorus stoichiometry at station ALOHA. *Deep-*
694 *Sea Research II,* 48, 1529–1566.
695
696 Keeling, C. D., Brix, H., & Gruber, N. (2004). Seasonal and long-term dynamics of the upper
697 ocean carbon cycle at station ALOHA near Hawaii. *Global Biogeochemical Cycles*, 18, GB4006,
698 doi:10.1029/ 2004GB002227.
699
700 Key, R.M., Olsen, A., van Heuven, S., Lauvset, S. K.. Velo, A., Lin, X., Schirnick, C., Kozyr,
701 A., Tanhua, T., Hoppema, M., Jutterström, S., Steinfeldt, R., Jeansson, E., Ishii, M., Perez, F. F.,
702 & Suzuki, T. (2015). Global Ocean Data Analysis Project, Version 2 (GLODAPv2).
703 ORNL/CDIAC-162, NDP-093. *Carbon Dioxide Information Analysis Center*, Oak Ridge
704 National Laboratory, US Dept.of Energy, Oak Ridge,Tennessee. doi:
705 10.3334/CDIAC/OTG.NDP093_GLODAPv2
706
707 Klausmeier, C.A., Litchman, E., Daufresne, T., & Levin, S.A. (2004). Optimal nitrogen-to-
708 phosphorus stoichiometry of phytoplankton. *Nature,* 429, 171–174.
709
710 Landing, W., Measures, C., & Resing, J. (2019). Profiles of dissolved trace elements collected
711 using a trace-metal clean rosette from surface to 1000m depth from two CLIVAR P16 cruises in

2005 and 2006. *Biological and Chemical Oceanography Data Management Office* (BCO-DMO), doi:10.1575/1912/bco-dmo.778403.1

Letelier, R.M., & Karl, D.M. (1998). *Trichodesmium* spp. physiology and nutrient fluxes in the North Pacific subtropical gyre. *Aquatic Microbial Ecology*, 15, 265-276.

Letscher, R. T., Moore, J. K., Teng, Y.-C., & Primeau, F. (2015). Variable C:N:P stoichiometry of dissolved organic matter cycling in the Community Earth System Model. *Biogeosciences*, *12*, 209–221. https://doi.org/10.5194/bg-12-209-2015.

Letscher, R.T., Primeau, F., & Moore, J.K. (2016). Nutrient budgets in the subtropical ocean gyres dominated by lateral transport. *Nature Geoscience*, 9, 815-819, doi: 10.1038/NGEO2812.

Martin, J.H., Knauer, G.A., Karl, D.M., & Broenkow, W.W. (1987). VERTEX: Carbon cycling in the northeast Pacific. *Deep-Sea Research A* 34, 2, 267–285.

Martiny, A. C., Pham, C.T.A., Primeau, F.W., Vrugt, J.A., Moore, J.K., Levin, S.A. & Lomas, M.W. (2013). Strong latitudinal patterns in the elemental ratios of marine plankton and organic matter. *Nature Geoscience*, 6**,** 279-283.

Martiny, A.C., Vrugt, J.A., & Lomas, M.W. (2014) Concentrations and ratios of particulate organic carbon, nitrogen, and phosphorus in the global ocean. *Scientific Data* 1:140048. http://dx.doi.org/10.1038/sdata.2014.48

Nicholson, D., Emerson, S., & Eriksen, C. C. (2008). Net community production in the deep euphotic zone of the subtropical North Pacific gyre from glider surveys. *Limnology and Oceanography*, 53, 2226–2236. https://doi.org/10.4319/lo.2008.53.5_part_2.2226

Olsen, A., Key, R.M., van Heuven, S., Lauvset, S.K, Velo, A., Lin, X., Schirnick, C., Kozyr, A., Tanhua, T., Hoppema, M., Jutterström, S., Steinfeldt, R., Jeansson, E., Ishii, M., Pérez, F.F., & Suzuki,T. (2016). The Global Ocean Data Analysis Project version 2 (GLODAPv2) – an internally consistent data product for the world ocean. *Earth System Science Data*, 8, 297–323, https://doi.org/10.5194/essd-8-297-2016.

Pelland, N. A., Eriksen, C. C., Emerson, S. R., & Cronin, M. F. (2018). Seaglider surveys at Ocean Station Papa: Oxygen kinematics and upper-ocean metabolism. *Journal of Geophysical Research*, *123*, 6408–6427. https://doi.org/10.1029/2018jc014091

Quay, P. (1997). Was a carbon balance measured in the equatorial Pacific during JGOFS?. *Deep-Sea Research II*, 44, 1765-1781.

Quay, P. D., & Stutsman, J. (2003). Surface layer carbon budget for the subtropical N. Pacific: δ13C constraints at Station ALOHA. *Deep Sea Research I*, *50*, 1045–1061, https://doi.org/10.1016/S0967-0637(03)00116-X

Quay, P., J. Cullen, W. Landing, and P. Morton (2015). Processes controlling the distributions of Cd and PO4 in the ocean, *Global Biogeochemical Cycles*, 29, 830–841, doi:10.1002/2014GB004998.

Quay, P., & Wu, J. (2015), Impact of end-member mixing on depth distributions of $\delta^{13}C$, cadmium and nutrients in the N. Atlantic Ocean, *Deep Sea Research II*, 116, 107-116, doi:10.1016/j.dsr2.2014.11.1109.

Quay, P., Emerson, S., & Palevsky, H. (2020). Regional pattern of the ocean's biological pump based on geochemical observations. *Geophysical Research Letters*, *47*, e2020GL088098. https://doi.org/10.1029/2020GL088098.

Redfield, A.C. (1958). The biological control of chemical factors in the environment. *American Scientist*, 46**,** 205-221.

Strom, S.L., Brady Olson, M., Macri, E.L., & Mordy, C.W. (2006). Cross-shelf gradients in phytoplankton community structure, nutrient utilization, and growth rate in the coastal Gulf of Alaska. *Marine Ecology*, 328, 75-92.

Takahashi, T., Sutherland, S. C., Wanninkhof, R., Sweeney, C., Feely, R. A., Chipman, D. W., et al. (2009). Climatological mean and decadal change in surface ocean *p*CO2, and net sea-air CO2 flux over the global oceans. *Deep Sea Research II, 56*, 554–577. https://doi.org/10.1016/j.dsr2.2008.12.009

Teng, Y-C., Primeau, F.W., Moore, J.K., Lomas, M.W. & Martiny, A.C. (2014). Global-scale variations of the ratios of carbon to phosphorus in exported marine organic matter. *Nature Geoscience*, 7, 895-898, doi: 10.1038/NGEO2303.

Wang, W-L., Moore, J.K., Martiny, A.C., & Primeau, F.W. (2019). Convergent estimates of marine nitrogen fixation. *Nature*, 566, 205-213, https://doi.org/10.1038/s41586-019-0911-2

Weber, T. & Deutsch, C. (2010). Ocean nutrient ratios governed by plankton biogeography. *Nature*, 467, 550-554.

Weber, T., Cram, J.A., Leung, S.W., DeVries, T., & Deutsch, C. (2016). Deep ocean nutrients imply large latitudinal variation in particle transfer efficiency. *Proceedings National Academy Sciences,* 113, 8606-8611.

Wong, C. S., Whitney, F. A., Crawford, D. W., Iseki, K., Matear, R. J., Johnson, W. K., Page, J.S., & Timothy, D. (1999). Seasonal and interannual variability in particle fluxes of carbon, nitrogen and silicon from time series of sediment traps at Ocean Station P, 1982–1993: Relationship to changes in subarctic primary productivity. *Deep-Sea Research II*, *46,* 2735–2760, https://doi.org/10.1016/S0967-0645(99)00082-X.

802 **Supporting Information**

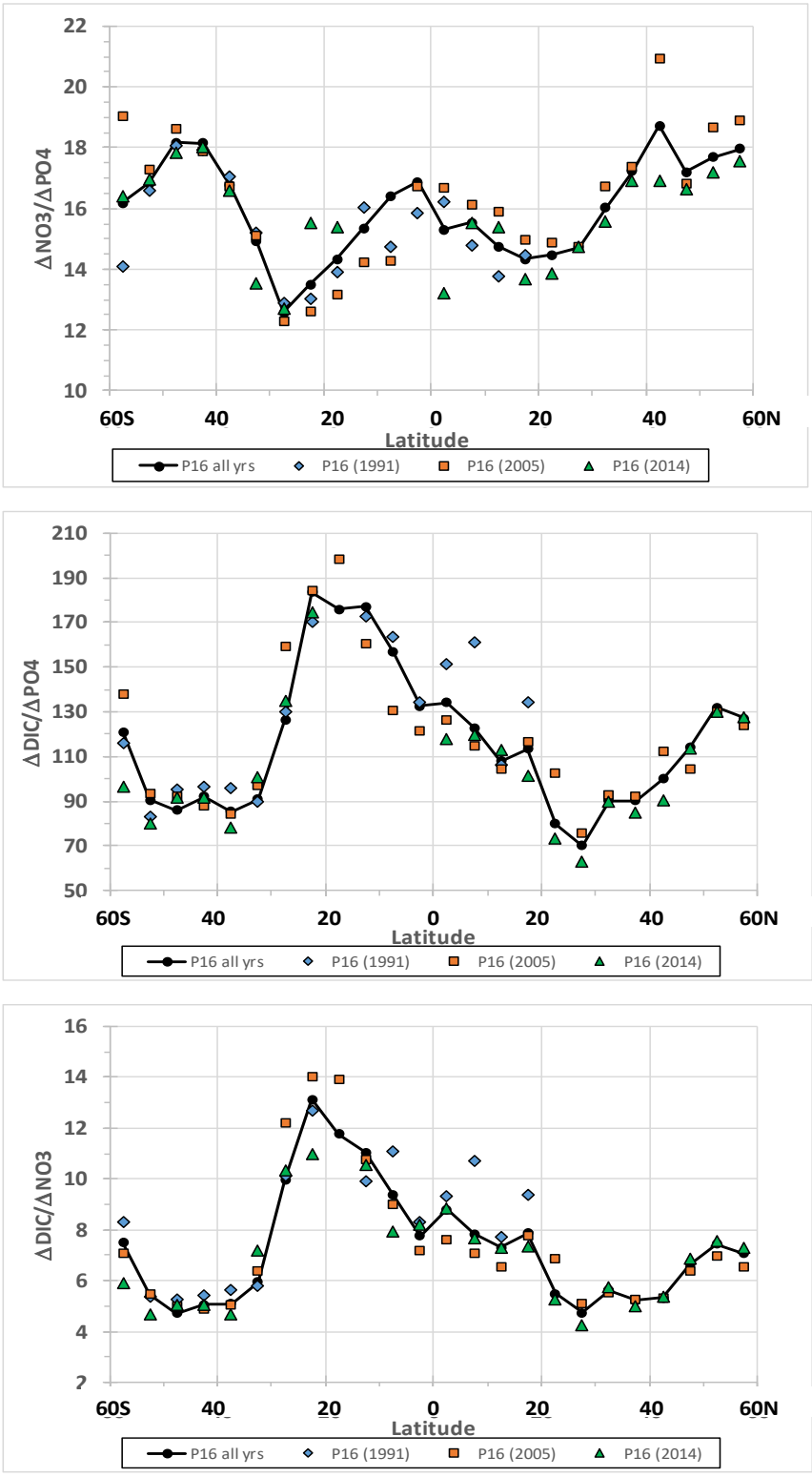

Figure S1. The regional trends in ratio of concentration depth gradients of ΔNO3/ΔPO4 (top), ΔDIC/ΔPO4 (middle) and ΔDIC/ΔNO3 (bottom) in the upper 300m using dissolved nutrient data from the reoccupation of individual GOSHIP-P16 cruises (along ~150°W) between 1991 and 2015. Black line is average of all cruises.

803

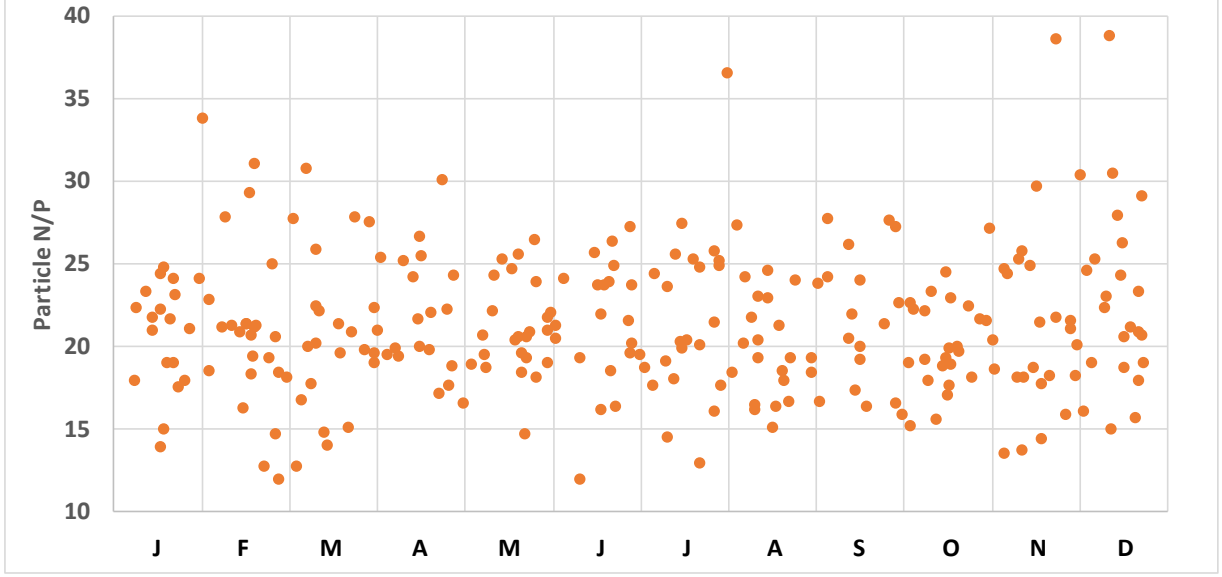

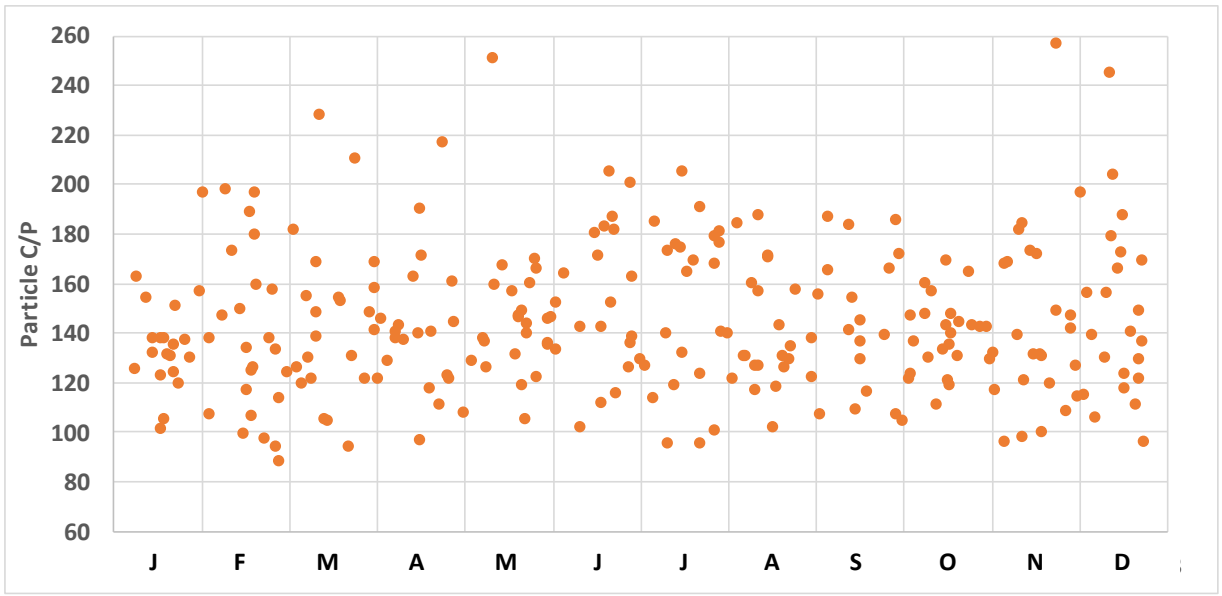

Figure S2. The N/P (top) and C/P (bottom) measured on suspended particulate organic matter collected in the upper at 100m at Stn ALOHA (23°N 153°W) between 1992 and 2018 and sorted by month. Particle elemental data for Stn. ALOHA was obtained via the Hawaii Ocean Time-series HOT-DOGS application.

804